JOURNAL OF ENVIRONMENTAL SCIENCES 94 (2020) 186–196

Available online at www.sciencedirect.com

ScienceDirect

www.elsevier.com/locate/jes

JES JOURNAL OF ENVIRONMENTAL SCIENCES

www.jesc.ac.cn

Comparative study on pyrolysis of bamboo in microwave pyrolysis-reforming reaction by binary compound impregnation and chemical liquid deposition modified HZSM-5

Haoran Du, Zhaoping Zhong, Bo Zhang, Kun Shi, Zhaoying Li*

Key Laboratory of Energy Thermal Conversion and Control of Ministry of Education, Southeast University, Jiangsu 210096, China

ARTICLE INFO

Article history:
Received 12 December 2019
Revised 11 March 2020
Accepted 12 March 2020
Available online 4 May 2020

Keywords:
Bamboo
Modified HZSM-5
Microwave
Binary compound impregnation
Chemical liquid deposition

ABSTRACT

The deactivation of catalyst is a significant reason for its limited application during the catalytic fast pyrolysis (CFP) process. To reduce the coke formation, binary compound impregnation (BCI) and chemical liquid deposition (CLD) were used to modify HZSM-5 catalysts. At the same time, the self-designed microwave reactor separated the pyrolysis of bamboo and catalytic upgrading of primary vapor, which made the catalytic effect more thorough. Experimental results indicated that CLD used TiO_2 deposition to cover external acid sites, while BCI by phosphorus-nickel could cover and partly destroy superficial acid sites through two different ways. Within the scope of the loaded amount studied, the yield of aromatic hydrocarbons in the oil phase increased at first and then decreased, while the coke formation reduced continuously. BTX (benzene, toluene and xylene), the most valuable product in bio-oil, drastically increased by 39.1% and 22.6% respectively over the CLD and BCI modified catalysts. Considering the catalytic performance as well as cost, CLD over HZSM-5 has more advantages in the CFP process to upgrade bio-oil.

Introduction

Biomass pyrolysis technology refers to the process by which feedstock is thermally decomposed into solid coke, pyrolysis gas and liquid bio-oil in an anoxic atmosphere (Dai et al., 2019). It is considered to be the industrially applicable biomass utilization technology with good application prospects. Catalytic fast pyrolysis (CFP), the most effective method to obtain high value-added biofuel product, plays a significant role in academic and industrial fields (Chen et al., 2015a; Ding et al., 2018; Luo et al., 2019). Among miscellaneous catalysts explored, HZSM-5 possesses unique pore structure, strong acidity and excellent thermal stability which performs wonderful shape-selective deoxidation action (Foster et al., 2012; Jae et al., 2011). It can effectively remove oxygenated substances in pyrolysis gas and form hydrocarbons during pyrolysis process (French and Czernik, 2010).

However, HZSM-5 aluminosilicate zeolite, as the acidic catalyst, is easy to enrich active components from the pyrolysis vapor on its surface, which polymerize on the external acid sites of catalyst and react to coke (Carlson et al., 2011; Jae et al., 2011). The main components of the coke formed during the pyrolysis process are macromolecular aromatic compounds (Derewinski et al., 2014; Song et al., 2010). They could not enter the interior of the HZSM-5 because of their large kinetic diameters but cover the outer surface, causing the blockage at the entrance to the aperture and the inactivation of catalyst (Du et al., 2013; Valle et al., 2012; Zhang et al., 2015a). Therefore, eliminating part of the external acid sites and retaining the internal acid sites of HZSM-5 catalyst at the same time be-

* Corresponding author.
E-mail: zzhong@seu.edu.cn (Z. Zhong).

https://doi.org/10.1016/j.jes.2020.03.014
1001-0742/

come the demand of researchers in this area. With this way, coke generation will decrease and higher production of target outcome will be obtained (Matias et al., 2008; Shao et al., 2017). Fortunately, some effective methods have been developed to optimize the superficial acid sites of HZSM-5 catalyst to retard the coke generation.

One method to adjust the acid site strength is loading some non-metallic elements to enhance the anti-coking properties of the catalyst. HZSM-5 modified by boron performed more efficiently in methanol olefin reaction and the coke of modified catalyst decreased (Yaripour et al., 2015). Meanwhile, phosphorus modified ZSM-5 obviously eliminated the strong acid sites and enhanced the hydrothermal stability of catalyst (Blasco et al., 2006; Derewinski et al., 2014). The aromatization reaction preferred to react on the strong acid sites of ZSM-5, while the alkylation reaction occurred on the weak acid sites more simply (Liu et al., 2010). At the same time, some transition metal elements, such as cobalt and molybdenum, were used to improve the catalytic performance of the catalyst (Liu et al., 2017). Some specialists also prepared HZSM-5 modified by zinc for the synthesis of aromatic hydrocarbons from ethylene, and found that its aromatization performance was significantly improved (Chen et al., 2015b). To reduce external coke amount and improve catalytic activity of HZSM-5, selectively inactivating the external acid sites of HZSM-5 catalyst was conducted through binary compound impregnation (BCI) method.

Another method is chemical liquid deposition (CLD) which covers the extra external acid sites of catalyst. To reduce the outward acidic sites deprived of changing the interior ones, silylation was probably one of the best methods (Zhang et al., 2015a; Zhao et al., 2016). During the silylation process, part of the modifiers (tetraethyl orthosilicate and methyl silicone oil) were absorbed on the surface of HZSM-5 by physical forces, and then converted to solid SiO_2 deposit by calcination (Dai et al., 2018). In the conversion from furan to *p*-xylene, HZSM-5 modified by CLD excellently enhanced 36% more selectivity of target production (Cheng et al., 2012). To further optimize product composition, tetrabutyl titanate (TBT) was used here to form TiO_2 deposit which was similar to SiO_2 but more catalytically active to catalyze feedstock. It was due to the unique weak superficial acidity of TiO_2, which mainly acted as a Lewis acidic center to perform strong selectivity for catalytic reactions (Hou et al., 2016; Kondoh et al., 2016; Li et al., 2010). In general, CLD is performed effectively in the area of biomass catalytic pyrolysis to obtain higher quality products because of its low cost, easy procedure and simple apparatus.

In recent years, microwave-assisted catalytic fast pyrolysis (MACFP) measure has achieved rapid development and application in biomass pyrolysis liquefaction, which was gradually conducted to pretreat biomass feedstock and manufacture pyrolytic biofuels (Borges et al., 2014; Du et al., 2013; Xie et al., 2014). Compared to conventional heating method, MACFP provided plenty of advantages, including high bio-oil yield, quick uniform self-heating, energy cost saving, simple operation and so forth. However, most experimental studies involved mixed catalyst and biomass feedstock together and pyrolyzed, which could not guarantee the catalyst catalyzes all raw materials. To solve this problem, the pyrolysis-reforming reaction separated biomass pyrolysis and primary pyrolysis gas catalytic upgrading process. All the vapors went through the catalyst fixed bed, which enhanced the effect of catalysts.

In this work, series of BCI and CLD modified HZSM-5 catalysts under different conditions were respectively prepared. The physicochemical characteristics of them were characterized by X-ray diffraction (XRD), N_2 physical adsorption analysis, NH_3 temperature programmed desorption (NH_3-TPD) and scanning electron microscopy (SEM), which sought reasons for catalytic performance improvement on the structure. Then, the original and modified catalysts were used in the self-designed microwave pyrolysis-reforming reaction, and the gas chromatography/mass spectrometry (GC/MS) investigated products contribution of bio-oil, especially for some kinds of mononuclear aromatics collectively called BTX (benzene, toluene and xylene). The ultimate goal of this study is to screen out modification methods with better performance.

1. Materials and methods

1.1. Materials

Bamboo was purchased at Huzhou in Zhejiang Province of China. It was crushed and sieved before the experiment to obtain powder with a particle size of about 120 mesh and then dried at 105°C for 48 hr to a constant weight. The proximate analysis results of bamboo were 71.42 wt.% volatile, 7.36 wt.% moisture, 2.94 wt.% ash and 18.28 wt.% fixed carbon. The ultimate analysis results of bamboo were 51.51 wt.% carbon, 6.12 wt.% hydrogen, 42.05 wt.% oxygen, 0.21 wt.% nitrogen and 0.11 wt.% sulfur. The parent HZSM-5 (Si/Al ratio = 27) was purchased from Nankai Catalyst Plant of China. Ammonium phosphate, nickel nitrate, ethyl alcohol absolute and tetrabutyl titanate were purchased from Sinopharm Group of China.

1.2. Catalysts preparation

1.2.1. Binary compound impregnation modified HZSM-5

Phosphorus modified HZSM-5 was prepared by wet impregnation method using $(NH_4)_3PO_4$ solution. HZSM-5 (5 g) was immersed into 10 mL aqueous solution of corresponding amount of $(NH_4)_3PO_4$ at 60°C for 4 hr, then it dried at 105°C for 12 hr, and finally calcined at 550°C for 4 hr. The phosphorus loading was ranged from 1.5 to 4.5 wt.% by controlling the amount of $(NH_4)_3PO_4$. And the phosphorus modified HZSM-5 catalysts were signified as x%P-HZ (x = 1.5, 2.5, 3.5, 4.5).

Nickel was loaded onto P-HZ catalyst by $Ni(NO_3)_2$ solution using the same method mentioned above. The slurry was dried for 12 hr at 105°C, and then calcined at 550°C for 4 hr to get the Ni-P-HZSM-5 catalyst. The catalysts that contained y wt.% (y = 1, 2, 3) of nickel were named as y%Ni-P-HZ. BCI modified HZSM-5 catalysts were obtained by two previous impregnation experiments.

1.2.2. Chemical liquid deposition modified HZSM-5

HZSM-5 (10 g) was dissolved into 100 mL ethyl alcohol absolute in a conical flask, and the modifier tetrabutyl titanate (TBT) was also added into the slurry with a water bath of 40°C for 4 hr. After reaction, liquid was evaporated by the rotary evaporator, and the obtained powder was placed in an oven to dry at 105°C for 12 hr, and ultimately calcined at 550°C for 4 hr in a muffle furnace. Different amounts of TBT were used in this process to prepare a series of catalysts with changed deposited amount. These catalysts that contained z wt.% (z = 2, 4, 8,12) of TiO_2 were named as z% TiO_2-HZ.

1.3. Physicochemical properties of catalysts

The XRD analysis was determined by the polycrystalline X-ray diffractometer (D8 Advance, Bruker, Germany) in the range of 5°–60° with a skimming speed of 6°/min at 40 kV to investigate the surface crystal phase structure of catalyst. The specific surface area and aperture analyzer (V-Sorb 2800TP, Gold APP Instrument Corporation, China) measured both the pore volume and the specific surface area of catalysts. The specific

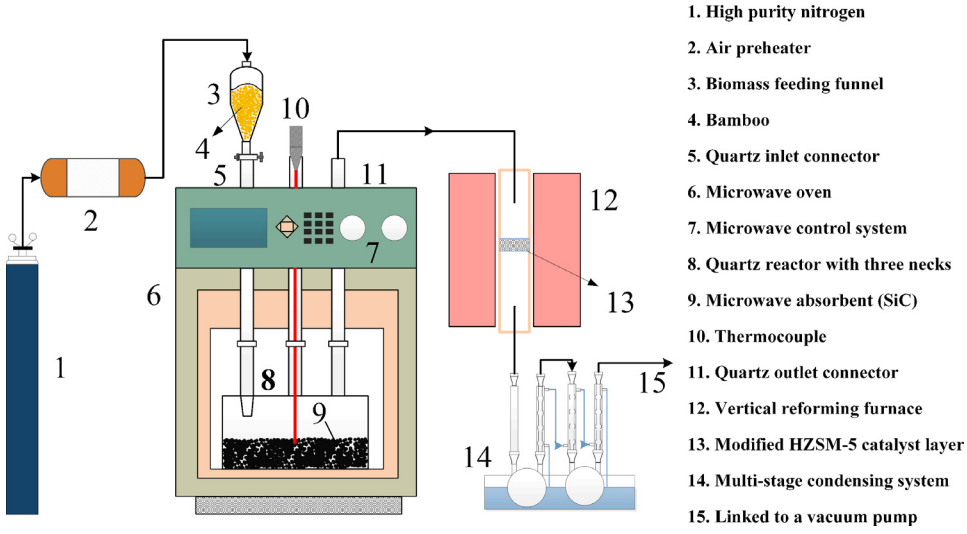

Fig. 1 – Schematic diagram of microwave pyrolysis-reforming reactor.

surface area (S_{BET}) was calculated by the Brunauer-Emmett-Teller (BET) equation, and the *t*-plot method calculated the micropore volume of catalysts. NH_3-TPD method measured the acidity of the catalyst, which used the chemical adsorption instrument (FineSorb 3010D, Finetec Instrument, China). The pretreated samples cooled from 450 to 80°C under the high-purity He environment for 1 hr. After pretreatment, the sample was saturated with NH_3 under N_2 gas environment, and then the physical absorbed NH_3 was blown out. Finally, the temperature was upraised from 100 to 600°C at a heating rate of 10°C/min, and instrument detected the NH_3 desorption signal during this process. SEM was performed to obtain the morphology analysis of HZSM-5 catalysts, which used the field emission scanning electron microscopy (QUANTA400, FEI, USA).

1.4. *Reactor*

The MACFP experimental reactor concluded the microwave oven (JHFWB-2S, Nanjing Jinhaifeng Microwave Technology Corporation, China) and a self-designed reforming furnace (maximum heating to 600°C). The reactor system (Fig. 1) was composed of (1) high purity nitrogen, (2) air preheater, (3) biomass feeding funnel, (4) bamboo, (5) quartz inlet connector, (6) microwave oven, (7) microwave control system, (8) quartz reactor with three necks, (9) microwave absorbent (SiC), (10) thermocouple, (11) quartz outlet connector, (12) vertical reforming furnace, (13) modified HZSM-5 catalyst layer, (14) multi-stage condensing system, and (15) linked to a vacuum pump to tow the pyrolysis gas out of the reactor.

The specific process of the experiment is as follows, 100 g of SiC were added into the quartz container at first to be used as the microwave adsorbent. SiC has good microwave absorption performance and can be easily heated to specified temperature. After that, the quartz reactor was placed in the hole of the microwave stove, and 10 g of modified catalyst was placed on the internal sieve of the reforming furnace. After connecting the quartz connectors, the reforming furnace and the condensing device, all the system was ventilated with nitrogen under 600 mL/min to vent the air. Finally, turn on the microwave reactor to increase the temperature. When the SiC bed and the reforming furnace were heated to the needed temperature (550 and 500°C respectively), 10 g of bamboo was added on the surface of heated SiC in the quartz container, which would be heated in two ways at the same time. One is the internal fast self-heating under the microwave environment; the other is the thermal conduction from the heated SiC. Pyrolysis reactions occurred in the microwave oven and the pyrolysis vapor passed through the heat preservation device into the reforming furnace to upgrade its composition. After the component optimization, the secondary pyrolysis gas was cooled by two stages of condensation to obtain bio-oil. Each experiment spent 45 min under the constant suction from the vacuum pump. With the intention of elevating the research reliability, each experiment was performed three times under the same conditions.

1.5. *Products analysis*

After each experiment, the catalysts have been used in the reforming furnace were carefully collected and dried in an oven at 120°C for 1 hr. Then, the dried samples were calcined at 650°C for 2 hr, and the coke yields were calculated based on the differences of mass. The char generation could be estimated based on the weight variances of the quartz reactor in the microwave oven cavity, and the entire solid product included coke and char two parts. The bio-oil production was calculated through the weigh difference of the condenser system after and before each experiment. Finally, follow the mass conservation calculation to attain the gas yield (gas yield = 100% - coke yield - char yield – bio-oil yield) (Zhang et al., 2015a).

The GC/MS instrument (7890A/5975C, Agilent, USA) analyzed the chemical compositions of each experimentally obtained bio-oil, which separated the heated gas phase by a HP-5MS (0.25 mm × 0.25 μm × 30 m) capillary column with the separation ratio of 1:10. High-purity He (99.999%) was used as the ambience gas (1.0 mL/min), and the programmed oven temperature was first at 40°C for 3 min, then increased to 180°C at a rate of 5°C/min and maintained for 2 min. Finally, it raised to 280°C at a heating rate of 10°C/min, and the whole process maintained 45 min. The National Institute of Standards and Technology (NIST) mass spectral data library distinguished each peak and filtered out each component of bio-oil.

1.6. *Data processing*

In the MACFP experiment, the relative content of the components in the pyrolysis product (R_{yield}) was defined as follows.

$$R_{yield} = P_s/P_{total} \times 100\% \quad (1)$$

Table 1 – Textural properties and coke yields of modified HZSM-5 catalysts.

Catalysts	S_{BET} (m^2/g)	S_{micro} (m^2/g)	$S_{external}$ (m^2/g)	V_{micro} (cm^3/g)	V_{meso} (cm^3/g)	Coke yield (%)
HZSM-5	354.11	291.23	62.88	0.134	0.073	11.13
1.5%P-HZ	283.06	229.58	53.48	0.116	0.081	10.06
2.5%P-HZ	255.01	209.74	45.27	0.096	0.080	8.85
3.5%P-HZ	224.52	180.70	43.82	0.081	0.084	7.95
4.5%P-HZ	201.73	161.27	40.46	0.076	0.081	6.48
1%Ni-2.5%P-HZ	249.91	203.58	46.33	0.095	0.070	8.67
2%Ni-2.5%P-HZ	244.61	198.34	46.87	0.094	0.083	8.51
3%Ni-2.5%P-HZ	239.01	192.12	46.89	0.094	0.089	8.33
2%TiO_2-HZ	346.35	279.71	66.64	0.131	0.075	8.93
4%TiO_2-HZ	337.41	268.24	69.17	0.128	0.075	7.58
8%TiO_2-HZ	322.52	250.96	71.56	0.127	0.077	6.34
12%TiO_2-HZ	305.69	233.73	71.96	0.125	0.078	6.01

S_{BET}: specific surface area calculated by Brunauer–Emmett–Teller (BET) method; S_{micro}, $S_{external}$, and V_{micro}: micropore surface area, external surface area, and micropore volume, respectively, calculated by t-plot method; V_{meso}: mesopore volume calculated by Barrett-Joyner-Halenda (BJH) method.

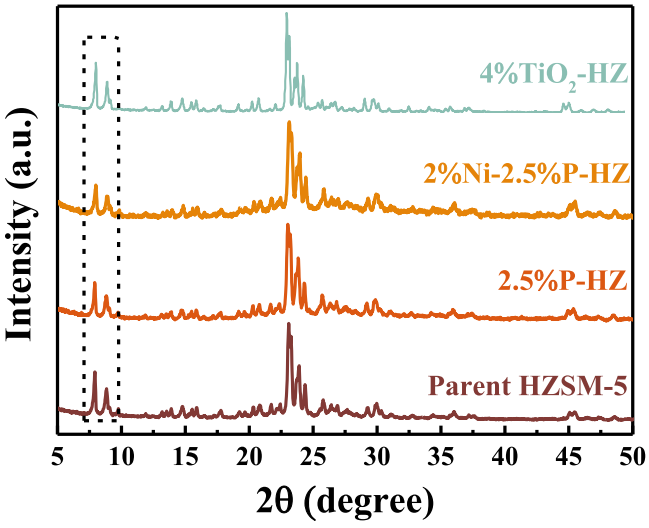

Fig. 2 – X-ray diffraction patterns of the parent and modified HZSM-5 (HZ). *x*%P-HZ: modified HZSM-5 catalysts with *x* wt.% of P; *y*%Ni-*x*%P-HZ: catalysts contained *y* wt.% of Ni; *z*%TiO_2-HZ: catalysts that contained *z* wt.% of TiO_2.

where P_s is the total peak area of one component and P_{total} is the total peak area of all products.

The selective of the monocyclic aromatic hydrocarbons (S_{ma}) was defined as follows.

$$S_{ma} = P_{ma}/P_{ah} \times 100\% \quad (2)$$

in which P_{ma} represented the total peak area of the monocyclic aromatic hydrocarbon in the pyrolysis product, and P_{ah} represented the total peak area of the aromatic hydrocarbon in the pyrolysis product.

2. Results and discussion

2.1. Physicochemical properties of catalysts

2.1.1. Phase structure characteristics of HZSM-5 catalysts

Fig. 2 shows the surface crystal structure of HZSM-5 catalysts via XRD. The diffraction patterns and the crystal structures were relatively complete and similar, which indicated that the surface coverage of P-Ni and the deposition of TiO_2 did not destroy the main framework of HZSM-5 catalyst. The peaks of $2\theta = 8°$ and 23° are X-ray characteristic diffraction peaks of HZSM-5 molecular sieve. The intensity of the low-angle characteristic diffraction peak after CLD was not much changed compared with the unmodified catalyst. This was because the precursor of TiO_2 had a large diameter and failed to enter the inside pore of the catalyst. Therefore, TiO_2 was primarily deposited on the external surface of the catalyst after calcination (Zhang et al., 2014, 2017). When the catalyst was loaded with phosphorus and nickel, the low-angle characteristic diffraction peak intensity and apparent crystallinity decreased, which was probably caused the partial structure damage by dealumination (Zhao et al., 2007; Zhuang et al., 2004).

At the same time, the obtained SEM results showed that the catalysts remained a relatively complete molecular sieve morphology after modification, which was consistent with the XRD results. Fig. 3 demonstrates the SEM images of HZSM-5, 2.5%P-HZ, 2%Ni-2.5%P-HZ and 4%TiO_2-HZ in order. As illustrated, the loading of phosphorus and nickel slightly roughened the external catalyst surface. However, the external surface of CLD modified HZSM-5 was dispersed with many fine particles, which were connected to each other and even stacked, making the external surface of CLD-HZSM-5 rougher than the BCI ones. This phenomenon indicated that a rough overlayer would form on the external surface of catalyst by CLD, while the small phosphorus molecules covered the surface more uniformly during BCI process, rather than being deposited as a block (Hou et al., 2016).

2.1.2. Porosity properties of catalysts

Table 1 shows the porosity and anti-coking properties of original and modified HZSM-5 catalysts. As illustrated, the BET surface area (S_{BET}), micropore surface area (S_{micro}), external surface area ($S_{external}$), micropore volume (V_{micro}) and mesopore volume (V_{meso}) are listed separately to present the varying tendency of catalyst porosity characteristics. It is obvious that as the phosphorus loading amount increased, the S_{BET}, S_{micro}, $S_{external}$ and V_{micro} of the catalysts decreased remarkably. This was because phosphorus addition affected the bridge hydroxyl of HZSM-5 structure, causing the partial destroy of catalyst framework. Meanwhile, the formation of phosphate species adhered into the inside of the pores resulting in the blockage of zeolite channels (Li et al., 2015). However, this downward trend gradually slowed down as the P loading amount increased. When the P load was small, there

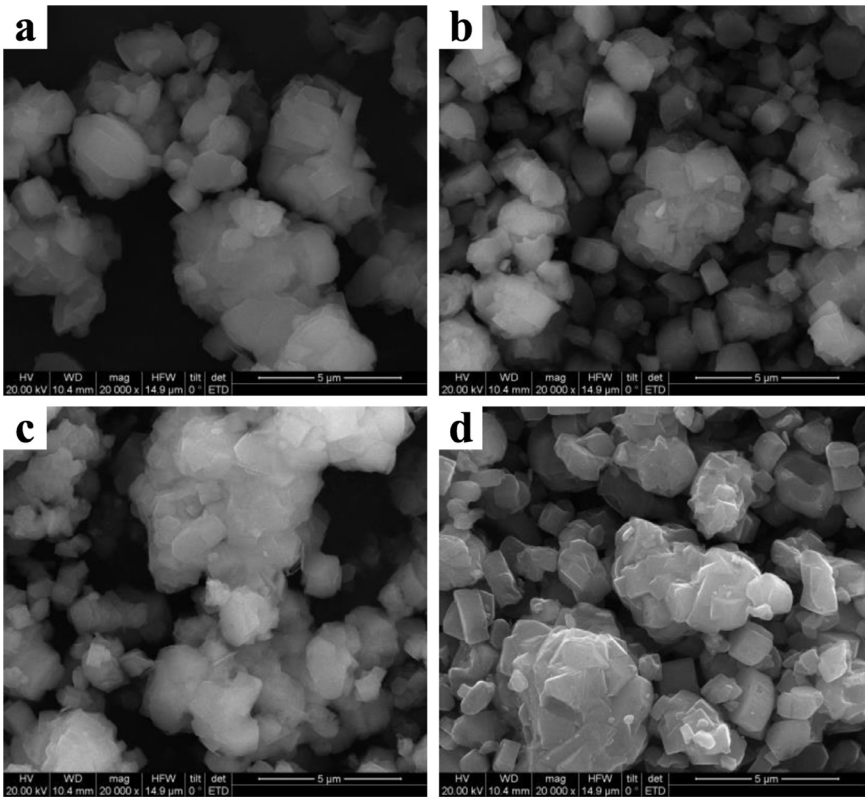

Fig. 3 – Scanning electron microscopy images of (a) HZSM-5, (b) 2.5%P-HZ, (c) 2%Ni-2.5%P-HZ, and (d) 4%TiO_2-HZ.

were enough active sites on the catalyst surface for phosphorus to bind, which would have a large impact on catalyst specific surface area. As the loading further elevated, phosphorus molecules failed to fully connect with the external surface of the catalyst, and the decreasing tendency became slower. At the same time, introducing Ni onto P-HZSM-5 could also cause the diversification of micropore volume and specific surface area. However, the decreasing effect of nickel on specific surface was extremely weak compared to phosphorus, while the micropore volume remained stable. The main reason is the nickel molecule is larger and mainly attaches on the external surface of catalyst.

In terms of CLD, as the growth of TiO_2 deposition, the S_{BET} and S_{micro} of modified catalysts decreased, while V_{micro} remained stable with a slight reduction. It indicated the deposited TiO_2 was mainly attached on the external surface of catalyst blocking partial pores, but had few effect on the internal micropore structure of HZSM-5 (Hou et al., 2016). On the other hand, the external rough overlayer of catalyst formed by TiO_2 deposition was possibly mesoporous structure, which slightly promoted increasing the value of $S_{external}$ and V_{meso}. Meantime, other researchers also proved the rough overlayer contained small mesopores (Gobin et al., 2011; Reitmeier et al., 2009). Besides, the blockage of pore mainly occurred at high-deposited amount. Therefore, it is necessary to control the amount of modifier added to create a suitable degree of coverage for catalyst. Comprehensively comparing these two methods, BCI has a more obvious shrinkage to the micropore due to its fractional destruction of the catalyst framework.

2.1.3. *Acidity characteristics of HZSM-5 catalysts*

The typical profiles with two desorption peaks were measured by NH_3-TPD method shown in Fig. 4a and b. The low temperature peaks at 216°C meant weak acidic sites, and the high temperature peaks at 450°C represented strong acid sites. For purpose of observing changes in acidity more clearly, strong and weak acid contents of different catalysts and their consistent peak temperatures are quantified and presented in Table 2. It was conducted by using standard samples, establishing the corresponding relationship between peak area and acid amount (mmol/g desorbed NH_3). Then, the distribution of strong and weak acidity of modified catalysts could be respectively calculated according to their integrated areas of the desorption peaks in the TPD profiles (Wang et al., 2015). With the increase of phosphorus loading from 0 to 4.5 wt.%, the total acidity of catalysts sharply undermined from 0.92 to 0.37 mmol/g after phosphorus impregnation especially for strong acidic sites as shown in Fig. 4a. Besides, the low temperature peaks that represented weak acid sites intensity slightly moved from 216°C to lower temperature (192°C) with the growth of loaded phosphorus amount. It is obvious that the intensity of strong acid sites declined far beyond weak acid sites, which could also be discovered from the ratio of strong acidity to total acidity (S/T). This value decreased from 0.48 of original HZSM-5 to 0.24 of 4.5%P-HZ, which demonstrated BCI modification eliminated the acid sites based on the acidic properties. Strong acid sites were the preferred binding targets for phosphorus atoms. The reason is that phosphorus addition does affect the bridge hydroxyl of HZSM-5 structure, causing partial aluminum environment of zeolites framework altered, and the acidic intensity of newly replaced phosphorus hydroxyl was lesser than that of aluminum hydroxyl (Derewinski et al., 2014).

Compared with phosphorus impregnation modification, which had the dual effect of covering and removing the acid sites of catalyst, CLD only optimized the surface structure by

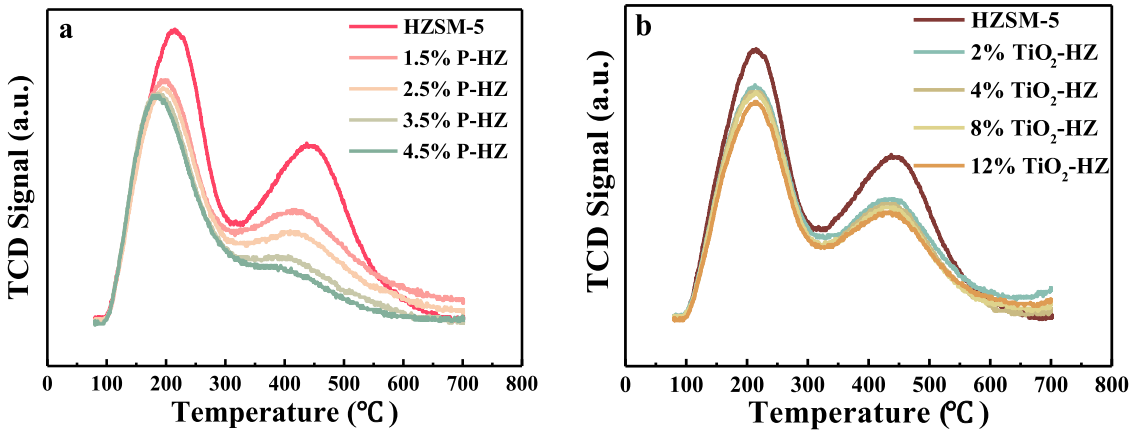

Fig. 4 – NH_3 temperature programmed desorption curves of the original and modified HZSM-5: (a) phosphorus modified HZSM-5 and (b) chemical liquid deposition (CLD) modified HZSM-5.

Table 2 – Acidity properties of original and modified HZSM-5 catalysts.

Catalysts	Weak acid sites		Strong acid sites		S/T	Total desorbed NH_3 (mmol/g)
	Peak temperature (°C)	Desorbed NH_3 (mmol/g)	Peak temperature (°C)	Desorbed NH_3 (mmol/g)		
HZSM-5	216	0.48	449	0.44	0.48	0.92
1.5%P-HZ	206	0.33	421	0.23	0.41	0.56
2.5%P-HZ	202	0.31	420	0.18	0.37	0.49
3.5%P-HZ	199	0.30	419	0.11	0.27	0.41
4.5%P-HZ	192	0.28	417	0.09	0.24	0.37
2%TiO_2-HZ	216	0.38	450	0.33	0.46	0.71
4%TiO_2-HZ	217	0.36	449	0.32	0.47	0.68
8%TiO_2-HZ	216	0.35	449	0.31	0.47	0.66
12%TiO_2-HZ	215	0.31	451	0.28	0.47	0.59

S/T: ratio of strong acidity to total acidity.

covering the external acid sites with deposits. In Fig. 4b, the both two-peak intensities of the 2%TiO_2-HZ were obviously lower than that of original HZSM-5, and the total acidity decreased from 0.92 to 0.71 mmol/g. However, with the TiO_2 deposition amount from 2 to 12 wt.%, the decline in acidity was getting slower just from 0.71 to 0.59 mmol/g, which indicated fewer acid sites were available on the external surface of the catalyst at high deposition. Compared to BCI treatment, the *S/T* value of HZSM-5 modified by CLD remained stable at around 0.46–0.48. This discover implied the CLD treatment covered the acid sites only based on the position of them, regardless of the acidic properties (Dai et al., 2018; Zhu et al., 2007). Meanwhile, the above characterizations clarified TiO_2 was mainly deposited on the external surface of catalyst. Therefore, a completion was concluded that TiO_2 largely located at the external surface of catalyst and eliminated the superficial acid sites.

2.1.4. *Anti-coking characteristics of HZSM-5 catalysts*

Studies have shown that polymerization occurs in the pores of HZSM-5 catalyst during pyrolysis process, which forms macromolecular aromatic compound (coke precursor) such as indene and naphthalene. This causes subsequent organics fail to enter the inside pores and have to attach on the external strong acid sites of catalysts to form coke (Dai et al., 2018; Du et al., 2016; Zhang et al., 2017). The coke yields of the modified catalysts decreased as the P and TiO_2 loading increased shown in Table 1, which indicated that the external acidity intensity was undermined by both two means. At the same time, the attachment of phosphorus atom inside the catalyst pores leaded to the reduction in aperture, which prevented the generated macromolecular organic matter from entering the pores to form a coke precursor. CLD achieved the same function by controlling the pore-opening size of HZSM-5. When the P load and TiO_2 deposition reached 4.5 and 12 wt.%, the coke yield reduced to 6.48% and 6.01%, respectively. However, too much loading and deposition would cause serious blockage of the pores and tremendously reduce the catalytic performance of HZSM-5. In general, BCI as well as CLD ultimately leaded to a decrease in the coke amount of the modified HZSM-5 catalysts, while Ni had little effect on catalyst coke reduction.

2.2. *Products distribution*

In the exploration for the efficient use of pyrolyzed biomass products, the generation and quality of bio-oil are equally significant. To obtain the high-valued bio-oil as much as possible, the influences of pyrolysis temperature and different modifications on bio-oil yield were investigated, as performed in Fig. 5. The noticeable varying tendency of pyrolyzed products was detected in Fig. 5a under the pyrolysis temperature from 450 to 650°C over original HZSM-5. With the temperature elevating, the liquid yield increased first and then decreased with the maximum value of 41.72% at 550°C. The volatile gas yield continually increased from 28.06% at 450°C to 39.20% at 650°C, while the solid phase yield continued to decline from 36.63%

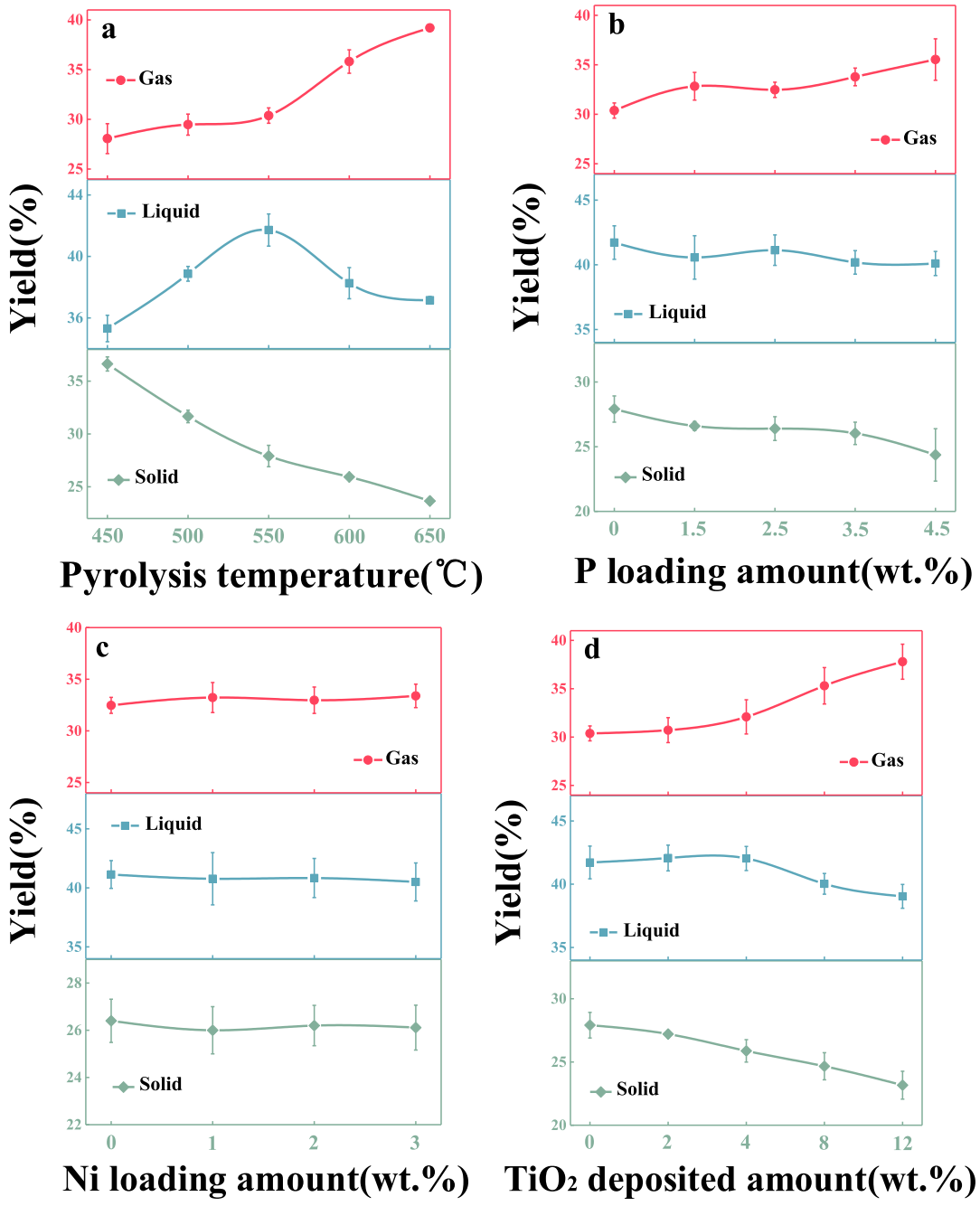

Fig. 5 – Products distribution of different (a) pyrolysis temperatures, (b) P loading amounts, (c) Ni loading amounts, and (d) TiO_2 deposited amounts.

to 23.65%. The main reason was that the higher the pyrolysis temperature was, the more exhaustively the feedstocks reacted, and the less the pyrolyzed char remained. Meantime, the higher pyrolysis temperature was easier for primary pyrolysis vapor to undergo secondary cracking and produce more non-condensable aeriform product, which was consistent with other previous studies (Wang et al., 2018). Therefore, the pyrolysis temperature of 550°C was performed in the subsequent studies to enhance the bio-oil yield.

However, various modifications of catalyst had little effect on the yield of pyrolyzed products, especially for bio-oil, which were shown in Fig. 5b, c and d in sequence. It is obvious that the oil-phase yields were fluctuated between 39% and 42%, and each value was the calculated average of three repeated experiments. In general, the bio-oil yields of BCI and CLD modification performed slight variation, which fluctuated within the error range. Therefore, only the compositions of oil-phase fraction were explored in the subsequent study.

2.3. *Catalytic performance of BCI modified HZSM-5 catalysts*

For the oil phase products obtained after microwave pyrolysis-catalyst reforming, the pyrolysis product components were analyzed by GC/MS and classified into three types consist of aromatics (BTX, naphthalene, indene), phenols and other

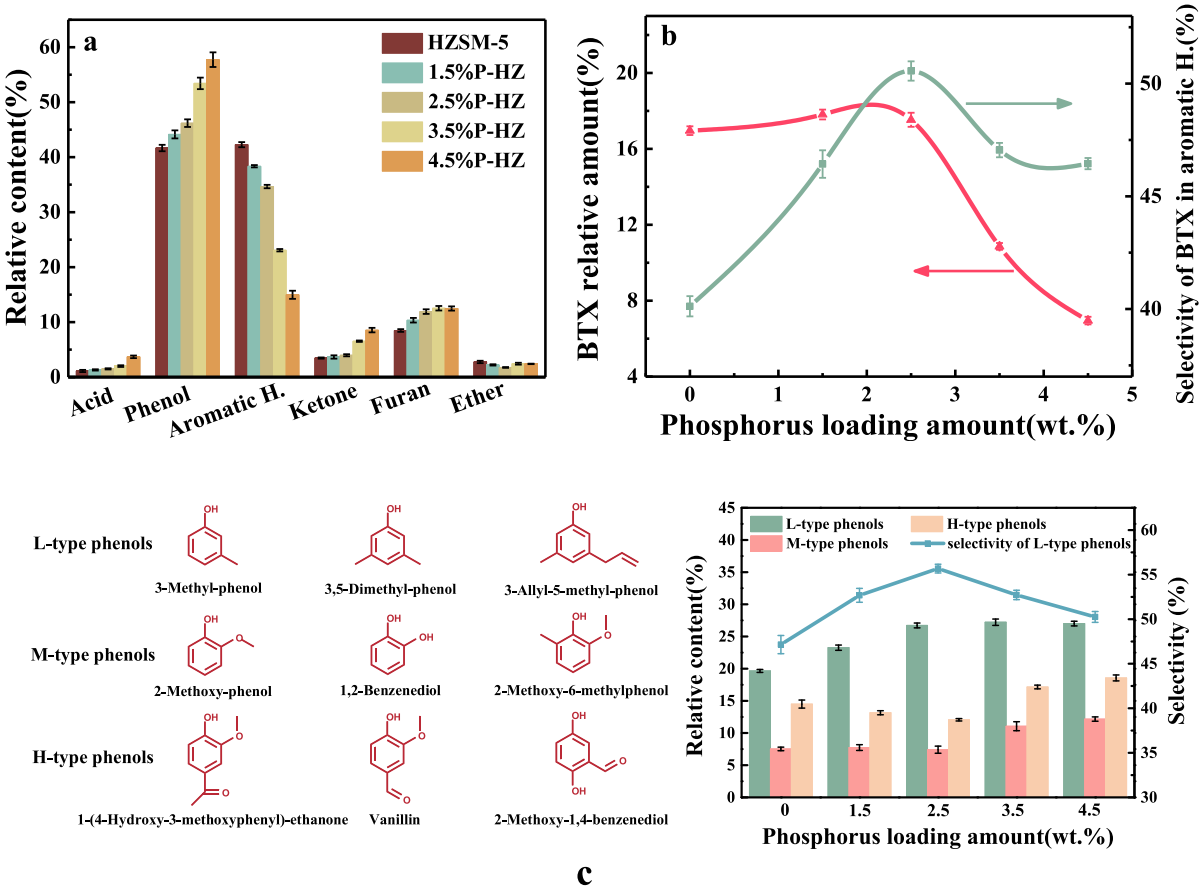

Fig. 6 – Compositions in oil fraction over modified HZSM-5 by phosphorus: (a) relative contents of different groups, (b) relative content and selectivity of BTX (benzene, toluene and xylene), and (c) relative contents of different phenols. L/M/H-type phenols: low/middle/high oxygen content type phenols; Aromatic H.: Aromatic hydrocarbon.

oxygen-containing molecules (acid, furan, ketone, ethers). At present, the aromatic hydrocarbon yield is one of the most important criterions for judging the performance of catalysts. Meanwhile, low oxygen content phenols can be converted into aromatic hydrocarbons by simple deoxidation, whose formation can also reflect the catalytic effect (Zhang et al., 2014). Therefore, investigating the alterations of the products distribution under BCI and CLD modification is meaningful. According to the oxygen content, phenols divided into low oxygen content type (L-type, benzene ring contains one oxygen atom on the side chain, such as methyl phenol, dimethyl phenol), middle oxygen content type (M-type, benzene ring contains two oxygen atoms on the side chain, such as dimethoxyphenol, methoxyphenol) and high oxygen content type (H-type, benzene ring contains three or more oxygen atoms on the side chain, such as methoxybenzene).

2.3.1. *MACFP performance over phosphorus modified HZSM-5 catalysts*

Fig. 6a and b presents the pyrolysis products contents, the relative amount and the selectivity of BTX of HZSM-5 modified by phosphorus respectively. With the P loaded amount increased from 0 to 4.5 wt.%, the relative content of aromatics decreased slowly at first and then had a sharp decline from 2.5 wt.%, while the relative content of phenols, acids and ketones inversely changed. In Fig. 6b, the selectivity as well as relative amount of BTX reached maximum value and then declined abruptly with growing P loaded quantity, whose maximum value were 50.56% and 17.53%, respectively at the 2.5 wt.% phosphorus loading amount. The relative yield of L-type phenols, which can be converted to aromatic hydrocarbons by one-step deoxygenation, also increased to the maximum at 2.5%P-HZ and then decreased as shown in Fig. 6c.

Since the peak intensity of strong acidic sites via NH_3-TPD and the corresponding coke yield decreased sharply after modification with the same trend. It is obvious that the coke and its forerunner are easier to generate at strong acidic sites. The impregnated P can uniformly cover the acidic sites on the apparent surface of the catalyst, and can connect with the silica-alumina framework in HZSM-5 resulting in the destruction of the strong acid sites, which reduced the external acid sites by two effects at the same time. The proper P loading caused somewhat catalyst pore blockage, which affected its catalytic activity and slightly reduced the aromatic hydrocarbon content. However, with the decrease of acid strength and the pore size, only smaller diameter molecule can access the interior of the catalyst resulting in the selectivity increase of the monocyclic aromatic hydrocarbons. Nevertheless, when the P loading was too large (more than 2.5 wt.%), the catalyst pores were severely blocked and the framework of HZSM-5 was partly destroyed, resulting in a sharp decrease of catalytic performance.

The entire tendency testified the phosphorus-loaded amount of 2.5 wt.% was the optimal qualification for maximum relative amount of BTX. At this loaded, specific surface area and micropore volume have noteworthy diversification

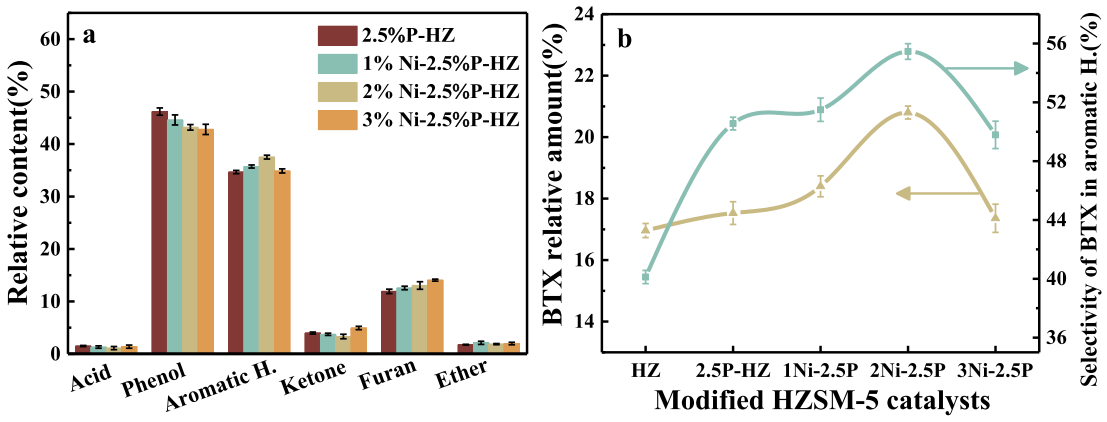

Fig. 7 – Compositions in oil fraction over modified HZSM-5 by binary compound impregnation (BCI): (a) relative contents of different groups and (b) relative content and selectivity of BTX. 2.5P-HZ: 2.5%P-HZ; yNi-2.5P: y%Ni-2.5%P-HZ.

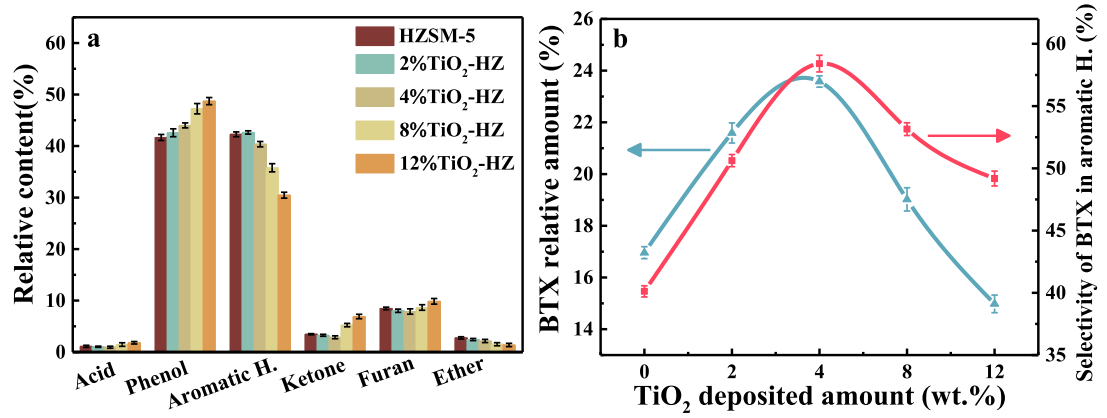

Fig. 8 – Compositions in oil fraction over modified HZSM-5 by CLD: (a) relative contents of different groups and (b) relative content and selectivity of BTX.

comparing with parent HZSM-5. Meanwhile, this change prevented the subordinate reaction from BTX to polycyclic aromatics, so the selectivity to BTX raised. Therefore, the 2.5%P-HZ was used for the subsequent process of BCI to optimize the surface catalytic activity by loading nickel.

2.3.2. *MACFP performance over nickel modified P-HZSM-5 catalysts*

Based on the optimal P loading of 2.5 wt.%, the effects of different Ni loadings on the catalytic performance of BCI modified HZSM-5 were investigated. Fig. 7 shows the product yields and selectivity of BTX in aromatic hydrocarbons over modified catalysts with different Ni loaded amounts. As shown in Fig. 7a, the aromatic yield first increases then decreases from 0 to 3 wt.% Ni loaded amount with the maximum value of 37.51% at 2%Ni-2.5%P-HZ, while the relative contents of ketones and acids show the opposite trend. At the same time, the relative contents of phenolic substances decreased with the increase of the load, and the furan substance slightly increased. As shown in Fig. 7b, with the increment of Ni loading, the relative amount as well as selectivity of BTX increased first and then decreased, meanwhile the maximum value of 20.80% and 55.46% were obtained at 2 wt.% Ni, respectively.

The trend of pyrolysis products presented that modification by nickel promoted the migration of hydrogen ions and the formation of carbon cations in the pyrolysis reaction. As a result, the hydrocarbons produced by bamboo pyrolysis underwent cyclization of carbon cations to form cyclic olefins. The aromatic hydrocarbon was finally formed under the next dehydrogenation on the nickel atoms, resulting in the improving aromatization performance of the catalyst (Cheng et al., 2015; Valle et al., 2010). At the same time, the introduction of Ni was beneficial to promote the decarbonylation in the pyrolysis process, resulting in the decrease of ketones. However, when the Ni amount further increased, the excessive loading caused the reduced catalytic activity, which was not conducive to the distribution of pyrolysis products. Therefore, 2%Ni-2.5%P-HZ was the best catalyst modified by BCI in studied range.

2.4. *Catalytic performance of CLD modified HZSM-5 catalysts*

Fig. 8a shows the products distribution of pyrolysis vapor under HZSM-5 catalysts modified by CLD with different TiO_2 deposition. It can be seen that the relative amount of aromatics first slightly raised to the top and then declined sharply from 4 to 12 wt.%, while the relative contents of ketones and furans changed in the opposite direction. A stable increment in relative amount of phenols occurred at the minor TiO_2 deposition (<4 wt.%), while a drastic rise happened as the TiO_2 deposition improved from 4 to 12 wt.%, which indicated that the excessive deposition could hinder the deoxygenation conversion process of phenols to aromatic hydrocarbons. The relative content and selectivity of BTX in the pyrolysis oil phase products of different CLD modified HZSM-5 catalysts are shown in Fig. 8b. Contrasted to the raw

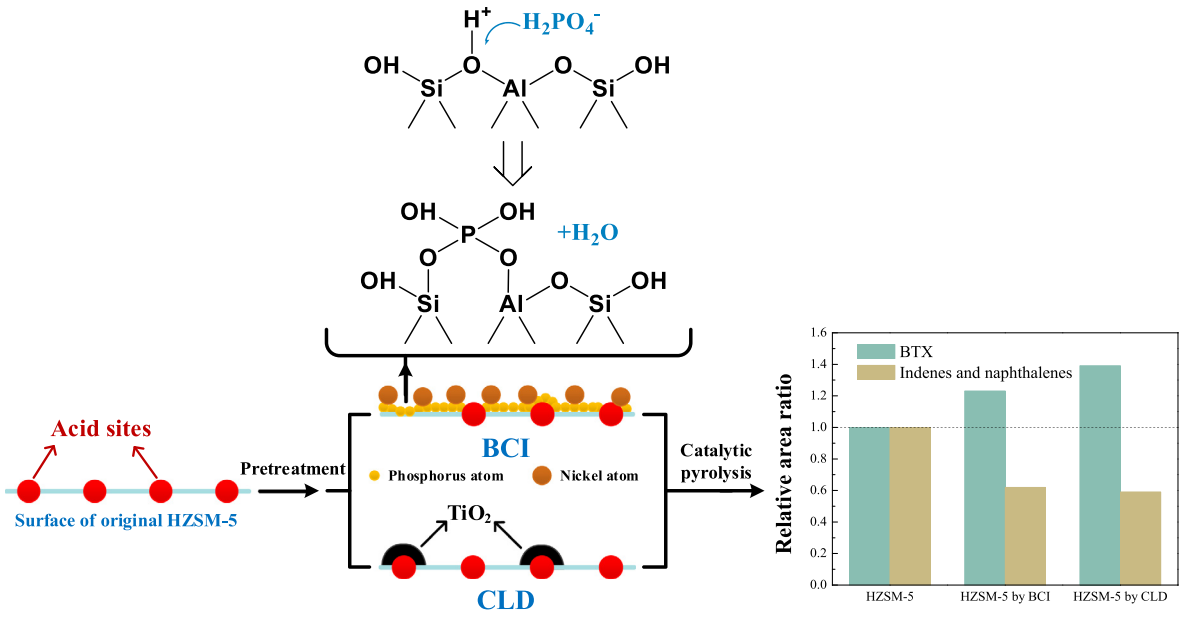

BCI: Cover and remove external acid sites by Binary Compound Impregnation
CLD: Cover external acid sites by Chemical Liquid Deposition

Fig. 9 – Schematic diagram of comparison of HZSM-5 catalysts for catalytic pyrolysis.

HZSM-5 catalyst, the CLD modified HZSM-5 catalysts made the relative content of BTX grow to the highest value of 23.58% at the TiO_2 deposition amount of 4 wt.%, and then decrease from 4 to 12 wt.%. At the same time, the selectivity of BTX in aromatic hydrocarbons performed the similar tendency, which also reached the maximum value of 58.41% at the 4 wt.% deposition. Therefore, the TiO_2 deposition of 4 wt.% became the optimal condition for MACFP experiment.

According to the studies, the kinetic diameters of BTX have approximate sizes with the pore-opening degree of HZSM-5, which well explained the shape-selective effect of the HZSM-5 catalyst especially for the generation of monocyclic aromatics (Zhang et al., 2015b). When the primary pyrolysis vapor of bamboo went across the layer of catalysts, it could spread into the interior apertures of catalyst and generate aromatics, because the framework of HZSM-5 owned the aromatics carbon pool (Ilias and Bhan, 2013). For original HZSM-5 catalyst, coke is more easily to generate compared to the modified one, which blocked the pore mouth and avoided the following catalytic reactions. For 2%TiO_2-HZ and 4%TiO_2-HZ, CLD treatment caused the partial coverage of external acidic sites, which played a significant role in decreasing the coke generation and optimizing the pore-opening size. Consequently, these two samples presented obviously improved catalytic performance compared to original HZSM-5. However, with the further increment of TiO_2 deposition (>4 wt.%), the pores of HZSM-5 were gradually blocked owing to the excessive deposition, which eventually leaded to the decrease of the aromatic hydrocarbons in pyrolysis products.

2.5. *Comparative analysis of BCI and CLD modified HZSM-5 catalysts*

During the microwave pyrolysis process, the yield and selectivity of BTX were strongly linked to the surface acidity and pore size of catalyst, which were the main purposes of both two methods to regulate. The two methods inhibited the excessive polymerization of the pyrolysis intermediate at acid sites, and improved the anti-coking performance of the catalyst by reducing surface acidity. Meanwhile, they optimized the pore size of HZSM-5 to enhance the deoxygenation reaction, because the catalysts with appropriate pore size had excellent deoxidation effect on the similar diameter reactants. In general, the small molecules like BTX are more likely catalytically generated by the BCI and CLD modified HZSM-5 catalysts.

The difference between BCI and CLD is the methods used to reduce the external acid sites and to regulate pore size of catalysts. The BCI method used phosphorus atoms to uniformly cover the acid sites on the surface of the catalyst, and to connect with the silica-alumina framework in HZSM-5 resulting in the destruction of the strong acid sites, which reduced the external acid sites by two ways at the same time. It adjusted pore volume and size by interior adhesion of phosphorus atoms and slight destruction of HZSM-5 framework. In contrast, CLD covered the superficial acid sites by depositing macromolecular TiO_2 on the external surface without any structure damage of catalyst. Meanwhile it only changed the pore-opening size of HZSM-5 to let more suitable oxygen-containing precursors enter into the catalyst for deoxygenation.

Fig. 9 shows the contrasting catalytic presentation of the BCI and CLD modified HZSM-5 catalysts, which explains the mechanism at the same time. MACFP of bamboo indicated that BTX contained in the bio-oil drastically increased by 39.1% and 22.6% respectively by using the CLD and BCI modified catalysts. Besides, the precursors of coke such as naphthalenes and indenes had a sharp decrease compared to original catalyst, which was also the main reason for coke decrement.

3. Conclusions

To explore the modification mechanism between BCI and CLD, they were contrastively used to modify HZSM-5 for CFP of bamboo in the microwave pyrolysis-reforming reaction. As

shown in the characteristic analysis, CLD caused the coverage of superficial acid sites and optimized pore-opening size at proper treating conditions. Whereas, BCI covered the external acid sites and destroyed partial strong acidic sites via connecting with the silica-alumina framework of HZSM-5. The chemical compositions in oil fraction indicated that BTX drastically increased by 39.1% and 22.6% respectively by using the CLD and BCI modified catalysts. In general, considering the catalytic performance and cost, CLD presented more efficient results compared to BCI in terms of obtaining high-quality products and decreasing coke generation.

Declaration of competing interest

The authors declare that they have no known competing financial interests or personal relationships that could have appeared to influence the work reported in this paper.

Acknowledgments

This work was supported by the National Key R&D Program of China (No. 2018YFB1501405) and the National Natural Science Fund Program of China (No. 51776042).

REFERENCES

Blasco, T., Corma, A., Martinez-Triguero, J., 2006. Hydrothermal stabilization of ZSM-5 catalytic-cracking additives by phosphorus addition. J. Catal. 237 (2), 267–277.
Borges, F.C., Du, Z., Xie, Q., Trierweiler, J.O., Cheng, Y., Wan, Y., et al., 2014. Fast microwave assisted pyrolysis of biomass using microwave absorbent. Bioresour. Technol. 156, 267–274.
Carlson, T.R., Cheng, Y.T., Jae, J., Huber, G.W., 2011. Production of green aromatics and olefins by catalytic fast pyrolysis of wood sawdust. Energy Environ. Sci. 4 (1), 145–161.
Chen, W.H., Lin, B.J., Huang, M.Y., Chang, J.S., 2015a. Thermochemical conversion of microalgal biomass into biofuels: a review. Bioresour. Technol. 184, 314–327.
Chen, X.C., Dong, M., Niu, X.J., Wang, K., Chen, G., Fan, W.B., et al., 2015b. Influence of Zn species in HZSM-5 on ethylene aromatization. Chin. J. Catal. 36 (6), 880–888.
Cheng, Y.T., Wang, Z.P., Gilbert, C.J., Fan, W., Huber, G.W., 2012. Production of p-xylene from biomass by catalytic fast pyrolysis using ZSM-5 catalysts with reduced pore openings. Angew. Chem. Int. Edit. 51 (44), 11097–11100.
Cheng, S.Y., Wei, L., Zhao, X.H., Huang, Y.B., Raynie, D.L., Qiu, C.L., et al., 2015. Directly catalytic upgrading bio-oil vapor produced by prairie cordgrass pyrolysis over Ni/HZSM-5 using a two stage reactor. AIMS Energy 3 (2), 227–240.
Dai, G.X., Wang, S.R., Huang, S.Q., Zou, Q., 2018. Enhancement of aromatics production from catalytic pyrolysis of biomass over HZSM-5 modified by chemical liquid deposition. J. Anal. Appl. Pyrolysis 134, 439–445.
Dai, L.L., Wang, Y.P., Liu, Y.H., Ruan, R., Duan, D.L., Zhao, Y.F., et al., 2019. Catalytic fast pyrolysis of torrefied corn cob to aromatic hydrocarbons over Ni-modified hierarchical ZSM-5 catalyst. Bioresour. Technol. 272, 407–414.
Derewinski, M., Sarv, P., Sun, X.Y., Muller, S., van Veen, A.C., Lercher, J.A., 2014. Reversibility of the modification of HZSM-5 with phosphate anions. J. Phys. Chem. C 118 (12), 6122–6131.
Ding, K., Zhong, Z., Wang, J., Zhang, B., Fan, L., Liu, S., et al., 2018. Improving hydrocarbon yield from catalytic fast co-pyrolysis of hemicellulose and plastic in the dual-catalyst bed of CaO and HZSM-5. Bioresour. Technol. 261, 86–92.
Du, S.C., Gamliel, D.P., Giotto, M.V., Valla, J.A., Bollas, G.M., 2016. Coke formation of model compounds relevant to pyrolysis bio-oil over ZSM-5. Appl. Catal. A-Gen. 513, 67–81.
Du, Z.Y., Ma, X.C., Li, Y., Chen, P., Liu, Y.H., Lin, X.Y., et al., 2013. Production of aromatic hydrocarbons by catalytic pyrolysis of microalgae with zeolites: Catalyst screening in a pyroprobe. Bioresour. Technol. 139, 397–401.
Foster, A.J., Jae, J., Cheng, Y.-T., Huber, G.W., Lobo, R.F., 2012. Optimizing the aromatic yield and distribution from catalytic fast pyrolysis of biomass over ZSM-5. Appl. Catal. A-Gen. 423-424, 154–161.
French, R., Czernik, S., 2010. Catalytic pyrolysis of biomass for biofuels production. Fuel Process. Technol. 91 (1), 25–32.
Gobin, O.C., Reitmeier, S.J., Jentys, A., Lercher, J.A., 2011. Role of the surface modification on the transport of hexane isomers in ZSM-5. J. Phys. Chem. C 115 (4), 1171–1179.
Hou, X., Qiu, Y., Zhang, X., Liu, G., 2016. Catalytic cracking of n-pentane over CLD modified HZSM-5 zeolites. RSC Adv. 6 (59), 54580–54588.
Ilias, S., Bhan, A., 2013. Mechanism of the catalytic conversion of methanol to hydrocarbons. ACS Catal. 3 (1), 18–31.
Jae, J., Tompsett, G.A., Foster, A.J., Hammond, K.D., Auerbach, S.M., Lobo, R.F., et al., 2011. Investigation into the shape selectivity of zeolite catalysts for biomass conversion. J. Catal. 279 (2), 257–268.
Kondoh, H., Tanaka, K., Nakasaka, Y., Tago, T., Masuda, T., 2016. Catalytic cracking of heavy oil over TiO_2-ZrO_2 catalysts under superheated steam conditions. Fuel 167, 288–294.
Li, J.W., Ma, H.F., Sun, Q.W., Ying, W.Y., Fang, D.Y., 2015. Effect of iron and phosphorus on HZSM-5 in catalytic cracking of 1-butene. Fuel Process. Technol. 134, 32–38.
Li, X.F., Shen, B.J., Xu, C.M., 2010. Interaction of titanium and iron oxide with ZSM-5 to tune the catalytic cracking of hydrocarbons. Appl. Catal. A-Gen. 375 (2), 222–229.
Liu, T.L., Cao, J.P., Zhao, X.Y., Wang, J.X., Ren, X.Y., Fan, X., et al., 2017. In situ upgrading of shengli lignite pyrolysis vapors over metal-loaded HZSM-5 catalyst. Fuel Process. Technol. 160, 19–26.
Liu, W.W., Hu, C.W., Yang, Y., Tong, D.M., Li, G.Y., Zhu, L.F., 2010. Influence of ZSM-5 zeolite on the pyrolytic intermediates from the co-pyrolysis of pubescens and LDPE. Energy Convers. Manag. 51 (5), 1025–1032.
Luo, Z.Y., Lu, K.Y., Yang, Y., Li, S.M., Li, G.X., 2019. Catalytic fast pyrolysis of lignin to produce aromatic hydrocarbons: optimal conditions and reaction mechanism. RSC Adv. 9 (55), 31960–31968.
Matias, P., Lopes, J.M., Laforge, S., Magnoux, P., Guisnet, M., Ribeiro, F.R., 2008. n-Heptane transformation over a HMCM-22 zeolite: catalytic role of the pore systems. Appl. Catal. A-Gen. 351 (2), 174–183.
Reitmeier, S.J., Gobin, O.C., Jentys, A., Lercher, J.A., 2009. Enhancement of sorption processes in the zeolite H-ZSM5 by postsynthetic surface modification. Angew. Chem. Int. Edit. 48 (3), 533–538.
Shao, S.S., Zhang, H.Y., Xiao, R., Shen, D.K., 2017. Catalytic conversion of furan to hydrocarbons using HZSM-5: Coking behavior and kinetic modeling including coke deposition. Energy Technol. 5 (1), 111–118.
Song, Z.X., Takahashi, A., Nakamura, I., Fujitani, T., 2010. Phosphorus-modified ZSM-5 for conversion of ethanol to propylene. Appl. Catal. A-Gen. 384 (1-2), 201–205.
Valle, B., Castano, P., Olazar, M., Bilbao, J., Gayubo, A.G., 2012. Deactivating species in the transformation of crude bio-oil with methanol into hydrocarbons on a HZSM-5 catalyst. J. Catal. 285 (1), 304–314.
Valle, B., Gayubo, A.G., Aguayo, A.T., Olazar, M., Bilbao, J., 2010. Selective production of aromatics by crude bio-oil valorization with a nickel-modified HZSM-5 zeolite catalyst. Energy Fuels 24 (3), 2060–2070.
Wang, J., Zhong, Z., Ding, K., Deng, A., Hao, N., Meng, X., et al., 2018. Catalytic fast pyrolysis of bamboo sawdust via a two-step bench scale bubbling fluidized bed/fixed bed reactor: Study on synergistic effect of alkali metal oxides and HZSM-5. Energy Convers. Manag. 176, 287–298.
Wang, S.R., Cai, Q.J., Chen, J.H., Zhang, L., Zhu, L.J., Luo, Z.Y., 2015. Co-cracking of bio-oil model compound mixtures and ethanol over different metal oxide-modified HZSM-5 catalysts. Fuel 160, 534–543.
Xie, Q.L., Peng, P., Liu, S.Y., Min, M., Cheng, Y.L., Wan, Y.Q., et al., 2014. Fast microwave-assisted catalytic pyrolysis of sewage sludge for bio-oil production. Bioresour. Technol. 172, 162–168.
Yaripour, F., Shariatinia, Z., Sahebdelfar, S., Irandoukht, A., 2015. Effect of boron incorporation on the structure, products selectivities and lifetime of H-ZSM-5 nanocatalyst designed for application in methanol-to-olefins (MTO) reaction. Micropor. Mesopor. Mater. 203, 41–53.
Zhang, B., Zhong, Z.P., Chen, P., Ruan, R., 2015a. Microwave-assisted catalytic fast pyrolysis of biomass for bio-oil production using chemical vapor deposition modified HZSM-5 catalyst. Bioresour. Technol. 197, 79–84.
Zhang, H., Luo, M., Xiao, R., Shao, S., Jin, B., Xiao, G., et al., 2014. Catalytic conversion of biomass pyrolysis-derived compounds with chemical liquid deposition (CLD) modified ZSM-5. Bioresour. Technol. 155, 57–62.
Zhang, H., Shao, S., Luo, M., Xiao, R., 2017. The comparison of chemical liquid deposition and acid dealumination modified ZSM-5 for catalytic pyrolysis of pinewood using pyrolysis-gas chromatography/mass spectrometry. Bioresour. Technol. 244, 726–732.
Zhao, G.L., Teng, J.W., Xie, Z.K., Jin, W.Q., Yang, W.M., Chen, Q.L., et al., 2007. Effect of phosphorus on HZSM-5 catalyst for C_4-olefin cracking reactions to produce propylene. J. Catal. 248 (1), 29–37.
Zhang, B., Zhong, Z.P., Xie, Q.L., Chen, P., Ruan, R., 2015b. Reducing coke formation in the catalytic fast pyrolysis of bio-derived furan with surface modified HZSM-5 catalysts. RSC Adv. 5 (69), 56286–56292.
Zhao, Y.W., Shen, B.X., Sun, H., 2016. Chemical liquid deposition modified ZSM-5 zeolite for adsorption removal of dimethyl disulfide. Ind. Eng. Chem. Res. 55 (22), 6475–6480.
Zhu, Z.R., Xie, Z.K., Chen, Q.L., Kong, D.J., Li, W., Yang, W.M., et al., 2007. Chemical liquid deposition with polysiloxane of ZSM-5 and its effect on acidity and catalytic properties. Micropor. Mesopor. Mater. 101 (1-2), 169–175.
Zhuang, J.Q., Ding, M., Gang, Y., Yan, Z.M., Liu, X.M., Liu, X.C., et al., 2004. Solid-state MAS NMR studies on the hydrothermal stability of the zeolite catalysts for residual oil selective catalytic cracking. J. Catal. 228 (1), 234–242.